

## Morphological analysis of isolated astrocytes using phase-contrast microscopy

© A.A. Shirokova<sup>1</sup>, E.V. Yakovlev<sup>1</sup>, I.V. Simkin<sup>1</sup>, N.A. Kolotieva<sup>1,2</sup>, S.V. Novikova<sup>1,2</sup>, A.D. Nasyrov<sup>1</sup>, I.R. Denisenko<sup>1</sup>, K.D. Gursky<sup>1</sup>, I.N. Shishkov<sup>1</sup>, D.E. Narzaeva<sup>1,2</sup>, A.B. Salmina<sup>1,2</sup>, S.O. Yurchenko<sup>1</sup>, N.P. Kryuchkov<sup>1</sup>

<sup>1</sup>Bauman Moscow State Technical University, Moscow, Russia

<sup>2</sup>Research Center of Neurology, Moscow, Russia

e-mail: shirokova2001@yandex.ru

Received May 03, 2024

Revised June 19, 2024

Accepted October 30, 2024

A new method of data collection and analysis for creating digital doubles of cellular systems is presented. To collect data, experiments were performed to visualize astrocyte growth for 18 days from the second day of cultivation. The obtained images were labeled and a Mask R-CNN neural network was trained based on them. From the detected astrocytes, features such as lengths of all astrocyte outgrowths  $L_i$ , number of nodes  $Nb_i$ , and total astrocyte area  $V_i$  were extracted. The obtained parameters were determined as functions of cultivation time. The obtained time dependencies will be used to create a digital twin of isolated astrocyte cells.

**Keywords:** digital twin, astrocytes, phase-contrast microscopy, machine learning.

DOI: 10.61011/EOS.2024.12.60446.6617-24

The production of new biomaterials remains a relevant objective in the biology field. For this purpose it is necessary to understand the processes in detail at the cellular level. Traditional experiments limit the research, therefore more and more attention is paid to digital twins — digital representations of real objects based on computer models and experimental data. The digital twins in cellular biology make it possible to describe the dynamics of cells [1], interaction of cells between each other [2,3], growth process [4–6] etc. The important area for development of a digital twin on the basis of computer modeling is a blood-brain barrier (BBB). It plays a critical role in support of the central nervous system, controlling the processes of metabolism, homeostasis, neuroinflammation, neuroplasticity and neurogenesis. Development of the BBB digital twin will help to accelerate and simplify the experiments, bring one closer to understanding the intercellular interactions in the brain. The first step for development of the BBB digital twin would be development of the astrocyte digital twin. Therefore, the study of the astrocyte growth process by methods of computer modeling is an important task for today. Astrocytes are star-like glial cells, widely available in the central nervous system (CNS). They play an important role in various CNS functions, such as maintenance of homeostasis of the intercellular space, metabolic control of neurovascular units, development and control of synaptic connections [7], response to neuroinjuries [8,9]. However, any computer model must be confirmed by experimental data.

For experimental studies of morphological signs of astrocytes, various microscopy methods are used, for example, electron [10], fluorescent [11,12], phase-contrast [13] etc.

However, most of these methods require a fixation procedure, and dead cells are being observed. Such method is not suitable for observation of the growth dynamics and changes in morphological features. For this purpose this paper uses phase-contrast microscopy.

Dissociated astrocyte culture obtained from newborn rats was used to conduct experiments to observe the growth of isolated astrocytes. Astrocytic culture was developed in CO<sub>2</sub>-incubator at temperature +37°C and relative humidity 98%. After formation of a monolayer, the culture was transferred into a 96-well plate.

Astrocyte morphology was studied using the method of phase contrast microscopy not requiring staining and fixation. Observations were carried out using visualization system „EVOS M7000“ (Thermo Fisher Scientific, USA). For 18 days the culture of astrocytes placed into the microscope incubator with a motorized stage was daily surveyed. Field of 5 × 5 frames (320 × 240 μm) with magnification ×40 in each of 60 well plate was observed daily.

Currently, to segment the images, convoluted neuron networks are used, since they demonstrate rather high precision. They are widely used in various objectives of physics [14], biology [15] etc. However, cell detection methods are created to detect the immunohistochemically stained and fixed cells, which is not suitable for the completed experiments. Therefore, to detect the isolated astrocytes, a neuron network model Mask R-CNN (regions with convolution neural networks) [16] was used, which was trained on our experimental data.

The neuron network was trained on images of astrocytes marked by LabelMe. More than 200 images 1024 × 1024

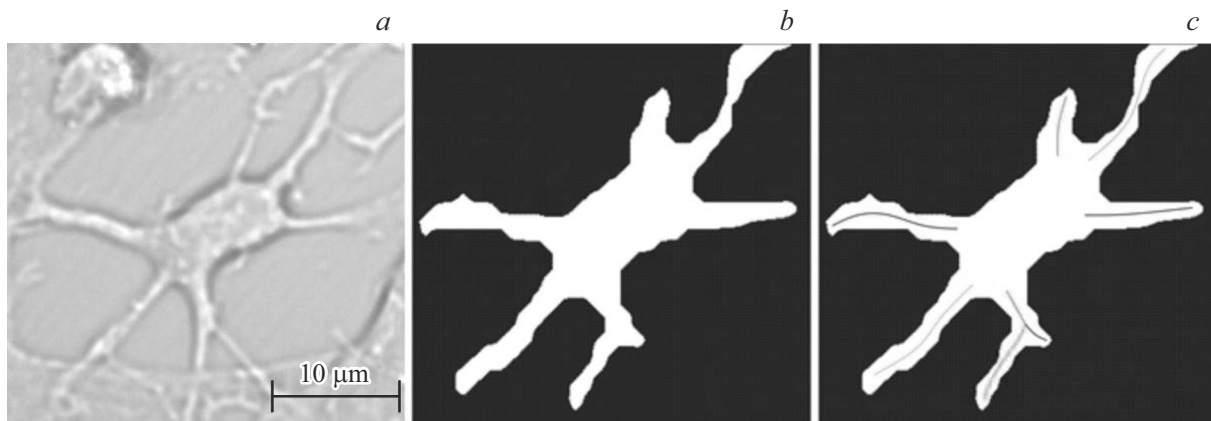


**Figure 1.** Astrocyte segmentation: (a) original image of astrocyte; (b) astrocyte detection by model 30; (c) segmented mask of astrocyte and its skeletonized branches, different colors comply with recognized segments.

obtained from source images divided into 4 parts were used for training. As a result, more than 1000 images obtained by expansion of the source data set using augmentation were used for training.

The obtained data set was used to train three models. Their main difference consists in resolution of the obtained image. Thus, model 20 inputs the image with resolution  $256 \times 256$  pixels, model 30 —  $512 \times 512$  pixels and model 50 —  $700 \times 700$  pixels. Numbers in the model names mean the number of thousands of steps for training. Model 20 had the worst characteristics among all models. Despite the fact that model 50 has highest precision ( $P = 0.72$ ), model 30 minimizes false positive results better. Therefore, for detection and further analysis of astrocytes model 30 was selected. The example of the astrocyte defined by the model is given in fig. 1, b.

To analyze the morphological features, three parameters were selected: total length of branches, number of branches and astrocyte area (including branches). To determine the astrocyte processes, first nuclei were extracted on the basis of the local isotropy of the image. After that the soma is removed from the mask, and the processes are exposed to skeletonization, as a result of which the processes remain with the thickness of one pixel. Then the number of segments (processes) is determined using the modernized graph method. The example of the determined processes is shown in fig. 1, c. Based on this result we identified nodes, processes and segments of processes, which made it possible to measure the dynamics of the cell growth in the experiment.

The post-treatment built histograms of astrocyte area distributions  $V_t$  on day 7, shown in fig. 2, and time dependences of process length  $Nb_t$  and number of nodes  $L_t$ , shown in fig. 3. As a result the total area of astrocytes was determined as function of lognormal distribution:

$$V_t = \frac{1}{x\sigma\sqrt{2\pi}} \exp\left(-\frac{(\ln x - \mu)^2}{2\sigma^2}\right),$$

where  $x$  — astrocyte area,  $\sigma = 0.42$  — standard deviation,  $\mu = 5.50$  — mathematical expectation.

Lengths of all astrocyte branches and number of nodes were determined as power functions of the dependence on the time of cultivation:

$$Nb_t = at^b,$$

where  $a = 2.30$ ,  $b = 0.27$  — coefficients determined from data approximation,

$$L_t = at^b,$$

where  $a = 36.1$ ,  $b = 0.07$  — coefficients determined from data approximation.

The experiments were done to visualize the primary culture of astrocytes using phase-contrast microscopy. The obtained images were marked and used to train the convoluted neuron network Mask R-CNN. Using the obtained model, we could measure such morphological parameters as the length of all astrocyte branches, the number of nodes and the total area of the astrocyte. It was established that (i) dependence of the total length of branches and their number on time is described by the power law,

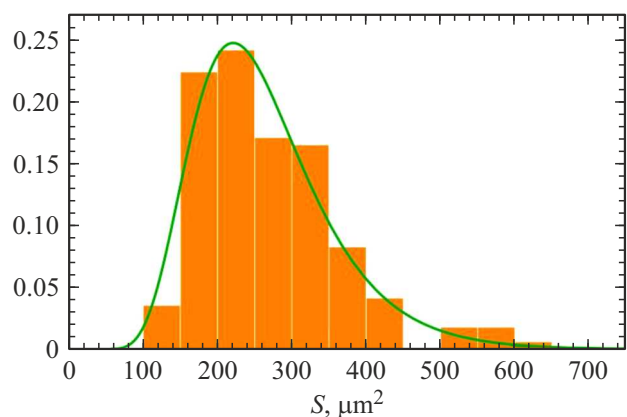


**Figure 2.** Histograms of astrocyte area distribution  $S, \mu\text{m}^2$ , measured on day 7 of the experiment, measured by model 30.

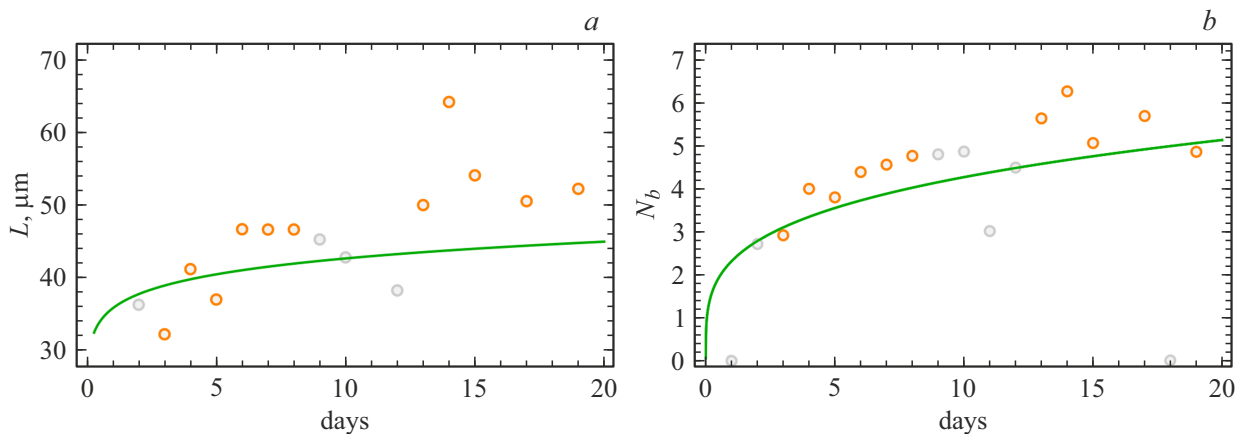


**Figure 3.** Dependences of astrocyte parameters on time: (a) average length of branches  $L$ ; (b) average number of nodes per astrocyte  $N_b$ , measured by model 30.

(ii) astrocyte distribution by size is subordinate to the Gaussian distribution.

Currently there are many papers on astrocyte detection and study of their dynamics. Thus, paper [17] demonstrates a new method to detect astrocytes based on DCNN. Despite the fact that the method makes it possible to relatively quickly and accurately detect astrocytes, it will not segment the produced images, therefore, it is not possible to detect their morphological parameters. Analysis of evolution of morphological parameters of cells was studied in other papers. Paper [18] developed a platform to study the dynamics of neurons, but neurons must be segmented manually.

Therefore, a method was developed, which makes it possible to detect astrocytes in low-contrast images and to identify their morphological features. The obtained data will be used to create digital twins of the isolated astrocyte cells, which will make it possible to detect various processes in the live systems without the need for experiments. Further it is planned to do experiments to observe the astrocytes after addition of various metabolites, and experiments with other cell cultures. The results obtained within the paper may be useful for scientific communities in the field of biology, biophysics, medicine, production of biomaterials.

### Funding

The paper was written with the support of the Russian Science Foundation grant №. 22-72-10128 at the Bauman Moscow State Technical University.

### Conflict of interest

The authors declare that they have no conflict of interest.

### References

- [1] J.A. Bull, F. Mech, T. Quaiser, S.L. Waters, H.M. Byrne. *PLoS Comput. Biol.*, **16** (8), e1007961 (2020). DOI: 10.1371/journal.pcbi.1007961
- [2] J. Metzcar, Y. Wang, R. Heiland, P. Macklin. *JCO Clin. Cancer Inform.*, **3**, 1–13 (2019). DOI: 10.1200/CCI.18.00069
- [3] G. Xu, H. Fang, Y. Song, W. Du. *Agriculture*, **13** (1), 142 (2023). DOI: 10.3390/agriculture13010142
- [4] M. Al Bakir, A. Huebner, C. Martínez-Ruiz, K. Grigoriadis, T.B.K. Watkins, O. Pich, D.A. Moore, S. Veeriah, S. Ward, J. Laycock, D. Johnson, A. Rowan, M. Razaq, M. Akther, C. Naceur-Lombardelli, P. Prymas, A. Toncheva, S. Hessey, M. Dietzen, E. Colliver, A.M. Frankell, A. Bunkum, E.L. Lim, T. Karasaki, C. Abbosh, C.T. Hiley, M.S. Hill, D.E. Cook, G.A. Wilson, R. Salgado, E. Nye, R.K. Stone, D.A. Fennell, G. Price, K.M. Kerr, B. Naidu, G. Middleton, Y. Summers, C.R. Lindsay, F.H. Blackhall, J. Cave, K.G. Blyth, A. Nair, A. Ahmed, M.N. Taylor, A.J. Procter, M. Falzon, D. Lawrence, N. Navani, R.M. Thakrar, S.M. James, D. Papadatos-Pastos, M.D. Forster, S.M. Lee, T. Ahmad, S.A. Quezada, K.S. Peggs, P. Van Loo, C. Dive, A. Hackshaw, N.J. Birkbak, S. Zaccaria, TRACERx Consortium, M. Jamal-Hanjani, N. McGranahan, C. Swanton. *Nature*, **616** (7957), 534–542 (2023). DOI: 10.1038/s41586-023-05729-x
- [5] M. Fujiwara, M. Imamura, K. Matsushita, P. Roszak, T. Yamashino, Y. Hosokawa, K. Nakajima, K. Fujimoto, S. Miyashima. *Curr. Biol.*, **33** (5), 886–898.e8 (2023). DOI: 10.1016/j.cub.2023.01.036
- [6] S. Loerakker, T. Ristori. *Curr. Opin. Biomed. Eng.*, **15**, 1–9 (2020). DOI: 10.1016/j.cobme.2019.12.007
- [7] E. Vezzoli, C. Cali, M. De Roo, L. Ponzoni, E. Sogne, N. Gagnon, M. Francolini, D. Braida, M. Sala, D. Muller, A. Falqui, P.J. Magistretti. *Cereb. Cortex*, **30** (4), 2114–2127 (2020). DOI: 10.1093/cercor/bhz226
- [8] Y. Zhou, A. Shao, Y. Yao, S. Tu, Y. Deng, J. Zhang. *Cell Commun. Signal.*, **18**, 1–16 (2020). DOI: 10.1186/s12964-020-00549-2
- [9] R. Siracusa, R. Fusco, S. Cuzzocrea. *Front. Pharmacol.*, **10**, 479091 (2019). DOI: 10.3389/fphar.2019.01114
- [10] S. Loerakker, T. Ristori. *Curr. Opin. Biomed. Eng.*, **15**, 1–9 (2020). DOI: 10.1016/j.cobme.2019.12.007

- [11] A. Horvat, M. Muhič, T. Smolič, E. Begić, R. Zorec, M. Krefit, N. Vardjan. *Cell Calcium*, **95**, 102368 (2021). DOI: 10.1016/j.cecca.2021.102368
- [12] R.V. Allahyari, K.L. Clark, K.A. Shepard, A.D.R. Garcia. *Sci. Rep.*, **9** (1), 565 (2019). DOI: 10.1038/s41598-018-37555
- [13] Y.C. Cheng, C.J. Huang, W.C. Ku, S.L. Guo, L.T. Tien, Y.J. Lee, C.C. Chien. *Stem Cell Rev. Rep.*, **18** (2), 839–852 (2022). DOI: 10.1007/s12015-021-10319-3
- [14] T. Lu, B. Han, F. Yu. *Ecol. Inform.*, **62**, 101277 (2021). DOI: 10.1016/j.ecoinf.2021.101277
- [15] F.R. Mashrur, A.D. Roy, D.K. Saha. In: 2019 4th Int. Conf. Electr. Inf. Commun. Technol. (EICT), IEEE (2019), pp. 1–5. DOI: 10.1109/EICT48899.2019.9068806
- [16] H.F. Tsai, J. Gajda, T.F. Sloan, A. Rares, A.Q. Shen. *SoftwareX*, **9**, 230–237 (2019). DOI: 10.1016/j.softx.2019.02.007
- [17] I. Suleymanova, T. Balassa, S. Tripathi, C. Molnar, M. Saarma, Y. Sidorova, P. Horvath. *Sci. Rep.*, **8** (1), 12878 (2018). DOI: 10.1038/s41598-018-31284-x
- [18] A. Mencattini, A. Spalloni, P. Casti, M.C. Comes, D. Di Giuseppe, G. Antonelli, M. D’Orazio, J. Filippi, F. Corsi, H. Isambert, C. Di Natale, P. Longone, E. Martinelli. *Patterns*, **2** (6), 100261 (2021). DOI: 10.1016/j.patter.2021.100261

*Translated by M.Verenikina*